

Improving molecularly imprinted nanogels by pH modulation

Zijie Zhang and Juewen Liu*

Department of Chemistry, Waterloo Institute for Nanotechnology

University of Waterloo, Waterloo, Ontario, N2L 3G1, Canada

Email: liujw@uwaterloo.ca

Abstract

Molecularly imprinted polymers (MIPs) are polymerized in the presence of a template molecule. After removing the template, the polymer scaffold can selectively rebind the template. Imprinting factor (IF) refers to the rebinding ratio of imprinted and non-imprinted polymers. Generally, the IF of most reported MIPs are still quite low (e.g. below 3.0). This is partially attributable to strong non-specific interactions. In this study, imprinted nanogels are prepared using two common dyes as templates, sulforhodamine B (SRhB) and fluorescein. By varying the buffer pH, non-specific electronic interactions between the template and the gels are reduced, leading to improved IF for the SRhB-MIPs from 1.5 (at pH 7.2) to 7.4 (at pH 9.0). At the same time, the binding capacity of the MIP remained similar. On the other hand, while pH tuning also improved the IF of the fluorescein-imprinted nanogels, the binding capacity dropped significantly. Using isothermal titration calorimetry (ITC), the SRhB-imprinted nanogels display a much higher affinity ($K_a = 2.9 \times 10^4 \text{ M}^{-1}$) than the non-imprinted ($K_a = 0.031 \times 10^4 \text{ M}^{-1}$) when rebinding is conducted in high pH (pH 9.0). This difference is mainly driven by enthalpy. This study suggests that pH tuning can be used to further improve MIPs.

Introduction

Molecular recognition is a fundamental process in chemistry and biology.¹ While many specific ligands are available, such as antibodies and aptamers,²⁻⁵ they are quite expensive and sometimes unstable. For certain applications such as environmental remediation, bulk quantity and cost-effective ligands are more desirable. To this end, molecularly imprinted polymers (MIPs) provide a useful alternative.⁶⁻⁸ To prepare MIPs, selected functional monomers are mixed with a target molecule to form a prepolymer,⁹ which is then polymerized in the presence of the target. The target might associate with the polymer using intermolecular forces such as hydrogen bonding,¹⁰ hydrophobic and electrostatic interactions.^{11, 12} Even after removing the template molecule, the recognition cavities still remain in shape for rebinding. Because of their low cost, robustness and straightforward synthesis, MIPs have been widely utilized for separations,^{13, 14} drug targeting,¹⁵⁻¹⁸ and biosensors.¹⁹⁻²¹

Despite these progresses, the imprinting factor (IF) is still quite low in general,²²⁻²⁸ typically in the range of 1.1-3.0 for a diverse range of targets including proteins,²²⁻²⁵ peptides, and small molecules.²⁶⁻²⁸ This is attributable to strong non-specific binding or weak specific binding. One potential method to improve the IF is by tuning buffer conditions, but success was still limited.²⁹⁻³² In this study, we included specific functional monomer to modulate molecular interactions. Sulforhodamine B (SRhB) and fluorescein are commonly used dyes for MIP. For example, the polymer formulation for imprinting SRhB has been previously optimized.^{33, 34} We herein prepare imprinted nanogels using these two dyes and report the effect of pH to significantly improve the IF. Compared to simple polymer chains, gels are useful for guest molecule loading, controlled release, and preparing stimuli-responsive materials.³⁵⁻³⁸

Experimental Section

Chemicals

Acrylamide (AAm), N-isopropylacrylamide (NIPAAm), methylene bisacrylamide (MBAAm), N-[3-(dimethylamino) propyl] methacrylamide (DMAPMA), allylamine, acrylic acid, SRhB, fluorescein sodium salt, and sodium dodecyl sulfate (SDS) were obtained from Sigma-Aldrich (St. Louis, MO). Ammonium persulfate (APS) and N,N,N',N'-tetramethylethylenediamine (TEMED) were from VWR (Mississauga, ON). Mill-Q water was used to prepare all the buffers and solutions. All other reagents and solvents were of analytical grade and used as received.

Preparation of imprinted and non-imprinted nanogels

The imprinted nanogels were prepared using the aqueous precipitation polymerization method.³⁹⁻⁴¹ Typically, AAm (29.1mg, 0.41 mmol), NIPAAm (46.4mg, 0.41 mmol), DMAPMA (3.4mg, 0.02 mmol), and the template molecule SRhB or fluorescein (5 μ M) were dissolved in phosphate buffer (20 mM, pH 7.2). The mixture was incubated for 30 min with slow stirring at 25 °C to form binding complexes. Then the cross-linker MBAAm (24.7mg, 0.16 mmol) and surfactant SDS (6 mg) were added. After purging the mixture with N₂ for 1 h, polymerization was initiated by adding APS (6 mg) and TEMED (3 μ L). The final reaction volume was 10 mL. The reaction was continued for 4 h at 25 °C under a N₂ atmosphere. The resultant imprinted nanogels were collected by centrifugation at 15,000 rpm for 5 min and then washed extensively using Milli-Q water and NaCl solution (0.2 M) until complete removal of the unreacted monomers and templates (confirmed by fluorescence spectrometry). The gels were frozen-dried for 24 h, and weighed to determine the reaction yield. The non-imprinted nanogels (NIPs) were prepared in the same way except that no template was added during polymerization.

Dynamic light scattering (DLS)

The ζ -potential and hydrodynamic size of the nanogels were measured by DLS (Zetasizer Nano ZS90, Malvern). To measure the ζ -potential at different pH values, the nanogels (50 $\mu\text{g}/\text{mL}$) were dispersed in 20 mM phosphate buffers ranging from pH 2.8 to 10.2. The temperature was maintained at 25 $^{\circ}\text{C}$ during measurement.

Rebinding assays

To determine the rebinding kinetics of the nanogels, 10 mg dried nanogels were suspended in 1 mL phosphate buffer (20 mM, pH 7.2). Then SRhB or fluorescein (5 μM) were added to the solutions and incubated at 25 $^{\circ}\text{C}$ for various periods of time. After centrifugation, the SRhB and fluorescein remained in the supernatants were diluted 100 times (final concentration < 50 nM) using the phosphate buffer and their fluorescence intensities (F) were determined (Ex = 565 nm and Em = 586 nm for SRhB; Ex = 460 nm and Em = 515 nm for fluorescein) using a microplate reader (Infinite F200Pro, Tecan). The intensities of 50 nM SRhB or fluorescein without nanogels were also determined as the initial fluorescence (F_0). The rebinding efficiency (%) was defined as $(F_0 - F)/F_0$. The IF was determined as the ratio of rebinding efficiencies between the imprinted and non-imprinted nanogels. To study the effect of pH, 10 mg dried nanogels were suspended in 1 mL phosphate buffer (20 mM) at different pH values to rebind 5 μM SRhB or fluorescein for 1 h at 25 $^{\circ}\text{C}$.

Isothermal titration calorimetry

Isothermal titration calorimetry (ITC) was performed using a VP-ITC Microcalorimeter (MicroCal). Prior to each measurement, each solution and suspension was degassed to remove air bubbles. To study the effect of pH, NIPs (10 mg/mL) or SRhB imprinted nanogels (SRhB-MIPs) in phosphate buffer solution (20 mM, pH 7.2 or 9.0) was loaded in 1.45 mL ITC cell at 25 $^{\circ}\text{C}$. In a syringe of 280 μL , SRhB

(100 μM) in the same pH buffer solution was titrated into the cell (10 μL each time). The first aliquot was used to correct volume errors on the first injection. The enthalpy (ΔH) and binding constant (K_a) were obtained through fitting the titration curves to a one-site binding model using the Origin software. The ΔG values were calculated using $\Delta G = -RT\ln(K_a)$, where R is the gas constant, while ΔS was calculated from $\Delta G = \Delta H - T\Delta S$.

Results and discussion

MIP formulation

In this work, fluorescein and SRhB were chosen as the template molecules (Figure 1). They both have high quantum yields, but emitting at different wavelengths. The emission of fluorescein is strongly pH dependent, while SRhB is pH insensitive. Fluorescein fluoresces most strongly in the double deprotonated state (pH >7.5), while the emission is significantly quenched by either single or double protonation.⁴² On the other hand, SRhB cannot be protonated in the normal pH range ($pK_a \sim 1.5$),⁴³ and is negatively charged at neutral pH.

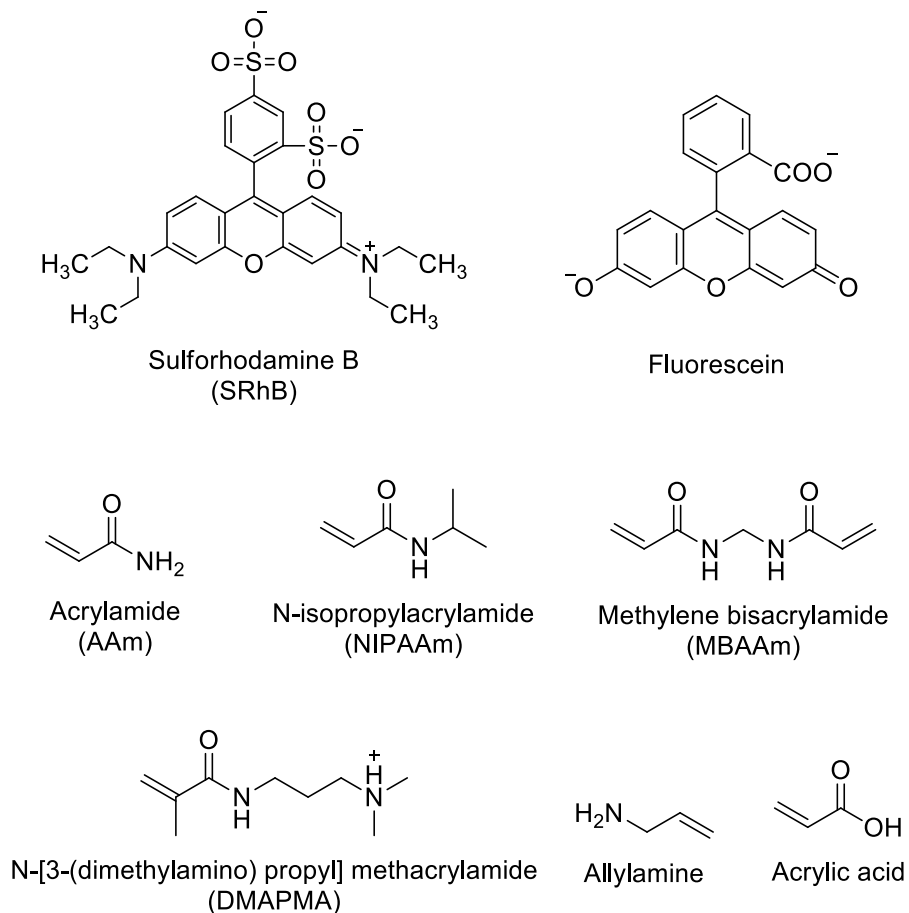


Figure 1. The structure of the two template molecules (SRhB and fluorescein) and the monomers and crosslinker used in this study.

Out of the many commercially available acrylic monomers, the following were chosen. First, since we intended to use precipitation polymerization to prepare nanogels, aside from acrylamide, a large fraction of the monomer was NIPAAm (see Figure 1 for structure), which displays the low critical solution temperature (LCST) property.⁴⁴ We prepare nanogels instead of monolithic gels to increase the surface area of our materials. Second, both target molecules are negatively charged at neutral pH. To achieve high binding affinity, cationic monomers are likely to be important for electrostatic attraction. Therefore, DMAPMA and allylamine were also tested. For comparison, a negatively charged monomer (acrylic

acid) was included as well. To achieve high specificity, we need to avoid too many positive charges. Therefore, these cationic monomers were tested at relatively low concentrations. Finally, MBAAm was used as the crosslinker, which is commonly used for MIP preparation.

In this study, we first tested nine gel formulations (Table 1) using SRhB as the template. The corresponding non-imprinted gel (NIP) were also prepared to determine the imprinting factor (IF). For the NIP preparation, the SRhB template was not added during polymerization. By comparing MIP formulations 1, 2 and 3 in Table 1, the IF increased with increasing percentage of acrylamide. This suggests that acrylamide might involve in the functional part of the imprinting process, or at least it can assist the arrangement of functional monomers. However, too much of acrylamide (e.g. 62 mol%) and thus too low of NIPAAm (20 mol%, MIP1) resulted in a low gel yield. From this study, 41 mol% acrylamide was determined to be optimal (MIP2). Table 1 also shows that the gel yield is significantly increased by using more crosslinkers MBAAm (MIPs 2, 4 and 5). However, too much crosslinkers resulted in a dense structure and lower IF. Therefore, we decided to use 16 mol% of the crosslinker.

Functional monomers are the most important part of MIPs. Table 1 indicates that MIPs containing 2 mol% positive monomers with suitable crosslinkers and other monomers displayed a high IF and high yield (MIP2, MIP6). On the other hand, negatively charged MIP7 showed a low IF, which can be rationalized by electrostatic repulsion with the template. In addition, although cationic MIPs favored high IF, too many positive charges also decreased the IF (e.g. comparing MIP2, 8 and 9). This is attributable to very strong non-specific electrostatic attractions with the template. After considering all these factors, we chose the MIP2 formulation for subsequent studies.

Table 1. Polymers formulation with different monomers tested for SRhB imprinting.

MIPs	Functional monomers						Yield (%w/w \pm SD)	Imprinti ng Factor (IF)
	NIPAAm (mol%)	AAm (mol%)	MBAAm (mol%)	DMAPMA	Allylamine	Acrylic		
				(mol%)	(mol%)	Acid (mol%)		
MIP1	20	62	16	2	0	0	24.6 \pm 1.3	1.87
MIP2	41	41	16	2	0	0	61.3 \pm 0.8	1.59
MIP3	62	20	16	2	0	0	58.7 \pm 1.1	1.24
MIP4	47	47	4	2	0	0	13.7 \pm 2.0	1.52
MIP5	34	34	30	2	0	0	63.5 \pm 1.9	1.12
MIP6	41	41	16	0	2	0	32.1 \pm 2.3	1.32
MIP7	41	41	16	0	0	2	19.75 \pm 1.2	1.03
MIP8	41	41	16	4	0	0	54.3 \pm 1.3	1.51
MIP9	41	41	16	8	0	0	49.7 \pm 0.7	1.25
NIP2	41	41	16	2	0	0	64.8 \pm 1.1	—

Gel characterization

Using our optimized gel formulation, we next prepared three batches of gels, respectively imprinted with fluorescein, SRhB, or without any template. After extensively washing, the resulting gels have an average size of 384 nm (NIPs), 389 nm (SRhB-MIPs) and 421 nm (fluorescein-MIPs) as characterized by DLS (Figure 2A). These gels can be easily dispersed in water, forming a stable dispersion.

To understand their surface charge, ζ -potential was measured as a function of pH (Figure 2B). Since DMAPMA is the only cationic monomer providing an amino group in the gels, ζ -potential reflects its

protonation state. For all the three gels, the ζ -potential goes from positive to negative between pH 9 and 10, which is consistent with the pK_a of DMAPMA being 9.2.⁴⁵

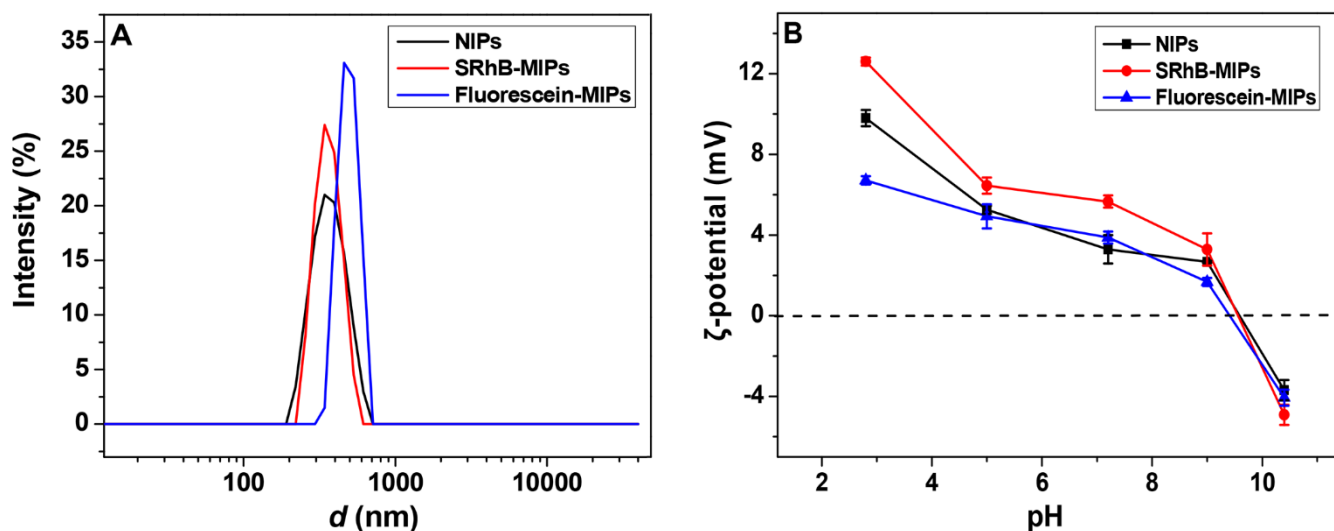


Figure 2. Characterization of the three types of nanogels by DLS. (A) Particle size distribution. (B) The ζ -potential of the nanogels as a function of pH.

Rebinding kinetics

We next studied the rebinding kinetics of the nanogels. To have a complete understanding, Nanogels (SRhB-1, SRhB-2, SRhB-3) were prepared at different SRhB concentrations (5, 10 and 50 μ M). The rebinding kinetics for SRhB are shown in Figure 3. All the MIP gels showed half adsorption in \sim 10 min. In comparison, the NIPs had a slower kinetics, reaching half saturation in \sim 30 min. The final adsorption capacity is also doubled for the MIP gels. For the three template concentrations, the one with the lowest template has the best rebinding performance.

To rationalize the above results, we did the following calculations. The yield of synthesis was calculated based on the dried gel product. With an average size of 384 nm, and a yield of 61.3%, the molar concentration of the gel particles during synthesis was ~ 4.69 nM (e.g. dispersing 6.13 mg gel in 1 mL of buffer). With 5 μ M template, each gel has around 1000 SRhB molecules if all the SRhB molecules are bound by the gels during synthesis. This appears to be an optimal density. When too many templates were used, template dimers and multimers may form,⁴⁶⁻⁴⁸ and thus the gel may deviate from the intended structure.

From this study we can also calculate the IF to be 1.59 for gel SRhB-1, where 5 μ M template was used. IF is defined as the ratio of rebound SRhB for the imprinted and non-imprinted gels. To achieve the best imprinting efficiency, we chose to use 5 μ M template for our subsequent experiments. For most of our subsequent assays, we used 10 mg/mL of nanogel (the same concentration as synthesis), and 5 μ M SRhB, so that the rebinding condition was similar to the synthesis condition.

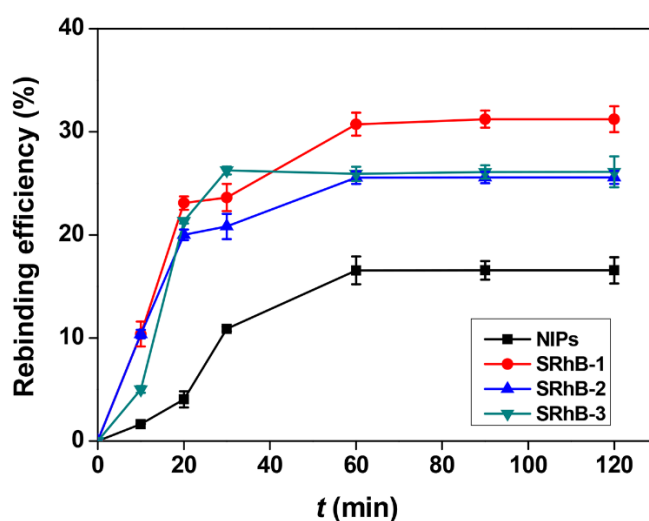


Figure 3. Rebinding kinetics of the three types of MIPs and the NIPs (10 mg/mL) for 5 μ M SRhB.

Effect of pH

Since both template molecules are negatively charged at neutral pH, and the gel formulation contained a cationic monomer, we suspect that pH might be important for rebinding. We next measured rebinding at different pH's. For the SRhB-templated gels, the rebinding efficiency was similar from pH 3 to pH 7.2 (the red bars, Figure 4A). Since the gels were made at pH 7.2 and the protonation state of the gel and the template does not change in this pH range, the rebinding efficiency is not affected. Interestingly, rebinding of SRhB to the NIP gels (black bars, Figure 4A) and to the gels imprinted with fluorescein (blue bars, Figure 4A) decreased significantly at high pH. Therefore, the IF was significantly improved at high pH (Figure 4C, red trace). Note that IF was calculated by the ratio of the red bars over the black bars in Figure 4A. This is attributed to the deprotonation of DMAPMA, whose pK_a is ~ 9.2 . At high pH, the gel became negatively charged to discourage non-specific SRhB binding. We conclude that the NIP gels bind SRhB mainly through electrostatic interactions while MIP gels have other interactions.

For comparison, the fluorescein-templated gels were also prepared and tested at various pH (Figure 4B). The highest rebinding efficiency of fluorescein took place at pH 7.2, where the gels were made and binding decreased sharply on both sides. At each pH, the cognate template, fluorescein, has the highest binding capacity.

The trend of IF change as a function of pH is completely inverted for the fluorescein imprinted gel (Figure 4C, blue trace); the best IF is achieved at lower pH. Although the MIP binding is significantly dropped at low pH, the NIP binding dropped even more (Figure 4B). For fluorescein, the effect of low pH is attributed to the protonation of fluorescein. At slightly basic conditions, fluorescein exists as a dianion with a high fluorescence quantum yield. Fluorescein has two pK_a values at 6.4 and 4.3, respectively. At pH 3, most fluorescein molecules are in the neutral form. The gel is positively charged at lower pH. Therefore, it appears that as fluorescein loses its negative charge, its interactions with both

NIP and MIP were weakened, suggesting the importance of electrostatic interaction. Despite that, the imprinted gel can still achieve a moderate binding based on other types of interactions, which likely are stemmed from the imprinting process. It needs to be pointed out that while the IF is high for the fluorescein-imprinted gels at low pH, the binding capacity is very low, making such gels less useful for practical applications.

On the high pH end, fluorescein does not change its protonation state and the changes must be related to the gel matrix (Figure 2B); that is the deprotonation of the DMAPMA monomer as discussed above. It is also interesting to notice that while the imprinted gel has the highest binding capacity, the pH-dependent trend is identical for all the three gels for fluorescein binding. Therefore, non-specific electrostatic interactions are quite significant for the imprinting of fluorescein.

Attempts to improve IF by changing buffer conditions including pH was explored previously.²⁹⁻³² However, the highest IF achieved was still just ~ 3.0 .^{29, 30} This can be explained by that the binding capacity of both their MIPs and NIPs changed similarly as pH was varied.²⁹ In our SRhB templated gels, the MIP capacity was not affected while the NIP capacity significantly decreased, leading to a much better IF at higher pH. This may be attributed to that we included a specific functional monomer (DMAPMA, $pK_a \sim 9.2$) in our gel formulation. At higher pH, non-specific charge interactions were more efficiently reduced but the specific interactions in the MIPs still maintained.

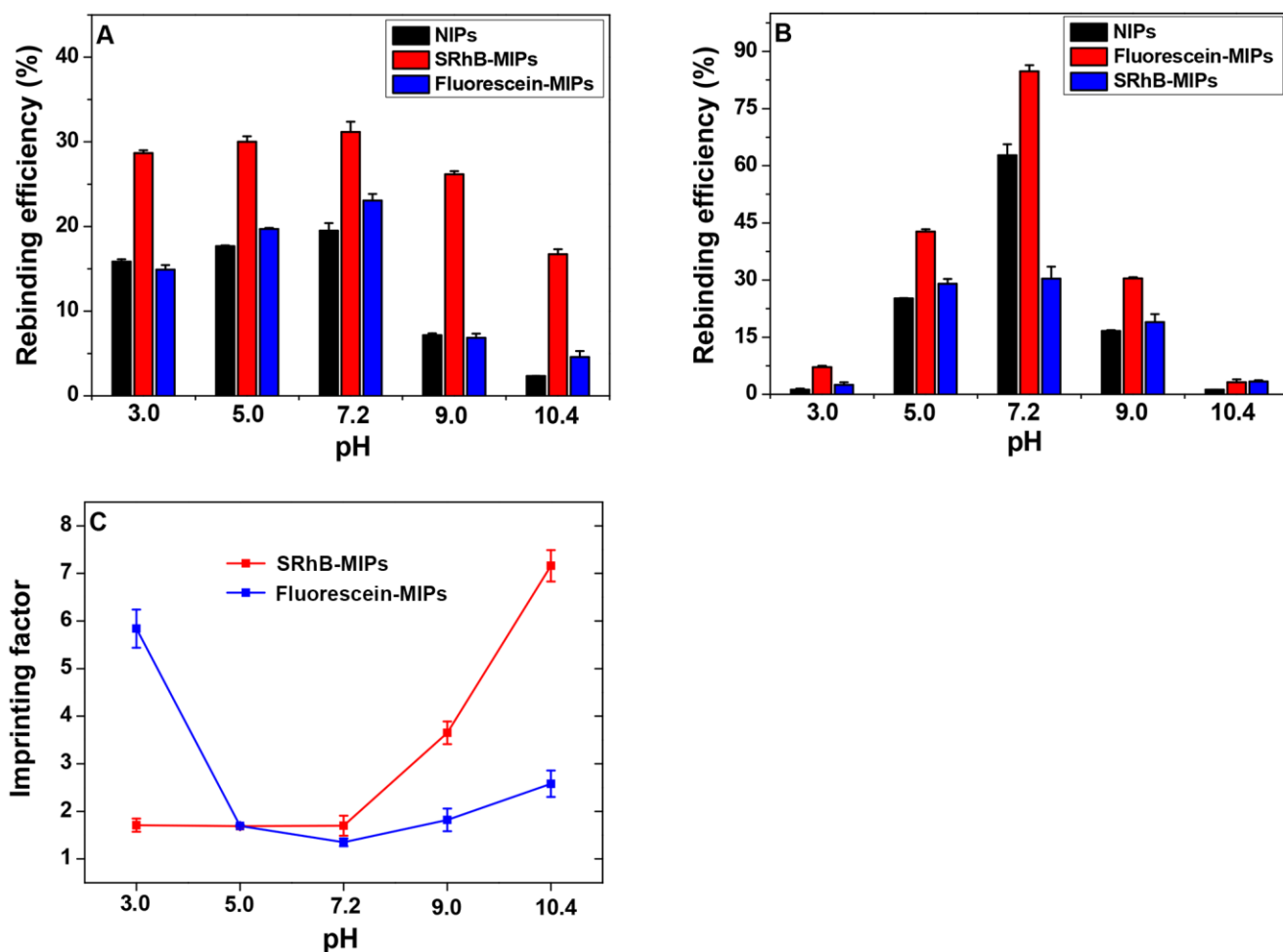


Figure 4. Effect of pH on rebinding efficiency of three types of nanogels for (A) SRhB and (B) fluorescein. (C) The IFs of the SRhB-MIPs and fluorescein-MIPs as a function of pH.

ITC analysis

Since the IF of SRhB-imprinted gels was significantly improved at high pH, and the binding capacity remained similarly high, tuning pH might be a useful way for improving MIPs. To understand the thermodynamic basis for such an improvement, isothermal titration calorimetry (ITC) was conducted. SRhB-imprinted gels were loaded into the ITC chamber and small volumes of SRhB were injected and the released heat was followed (Figure 5A). We chose pH 9.0 and pH 7.2 for high and low pH,

respectively. Fluorescein imprinted gels were not tested since the binding capacity was significantly decreased at high or low pH.

As shown in Figure 5A, the SRhB-imprinted gels showed a similar heat release at both pH 7.2 and 9.0, which is consistent with the fluorescence-based binding assays. On the other hand, the amount of heat release was significantly lower for the NIP gels (Figure 5B). In particular, at pH 9.0, barely any heat was released. The ΔH of SRhB-MIPs was around 24 kcal/mole (pH 7.2 and 9.0), while for the NIPs only 15 kcal/mole at pH 7.2 and 8 kcal/mole at pH 9.0. SRhB-MIPs also have higher binding affinity with a K_a of $0.47 \times 10^5 \text{ M}^{-1}$ at pH 7.2 and $0.29 \times 10^5 \text{ M}^{-1}$ at pH 9.0, which are much larger than those of the NIPs (Table 2). Therefore, imprinting has created binding sites for SRhB that are enthalpy favored. It is interesting to note that the entropy effect has largely compensated the gain made in the enthalpy term. The results further proved our successful imprinting of SRhB-MIPs with higher affinity and capacity from the thermodynamics aspect.

ITC has been used to characterize MIP binding in a few cases.⁴⁹⁻⁵² For example, a special-designed fluorescently-labeled MIP gave a K_a of $4.3 \times 10^5 \text{ M}^{-1}$ ($\Delta G = -7.7$ kcal/mole) by ITC when rebinding for small template molecules.⁴⁹ A protein-resemble MIP selectively rebinding its template yielded a $\Delta G = -8.4$ kcal/mole.⁵⁰ ITC data for MIP binding were also used to discriminate epimeric disaccharides, in which $K_a = 0.025 \times 10^5 \text{ M}^{-1}$, $\Delta H = -8.92$ kcal/mole for D-lactulose while $K_a = 0.058 \times 10^5 \text{ M}^{-1}$, $\Delta H = 8.95$ kcal/mole for D-lactose.⁵¹ These thermodynamic values are comparable with our ITC measurements. It is interesting to note that binding performance by NIPs was rarely been studied by ITC. We herein obtained a set of values for our NIPs ($K_a = 0.0031 \times 10^5 \text{ M}^{-1}$, $\Delta G = -3.3$ kcal/mole), consistent with the enhanced IFs.

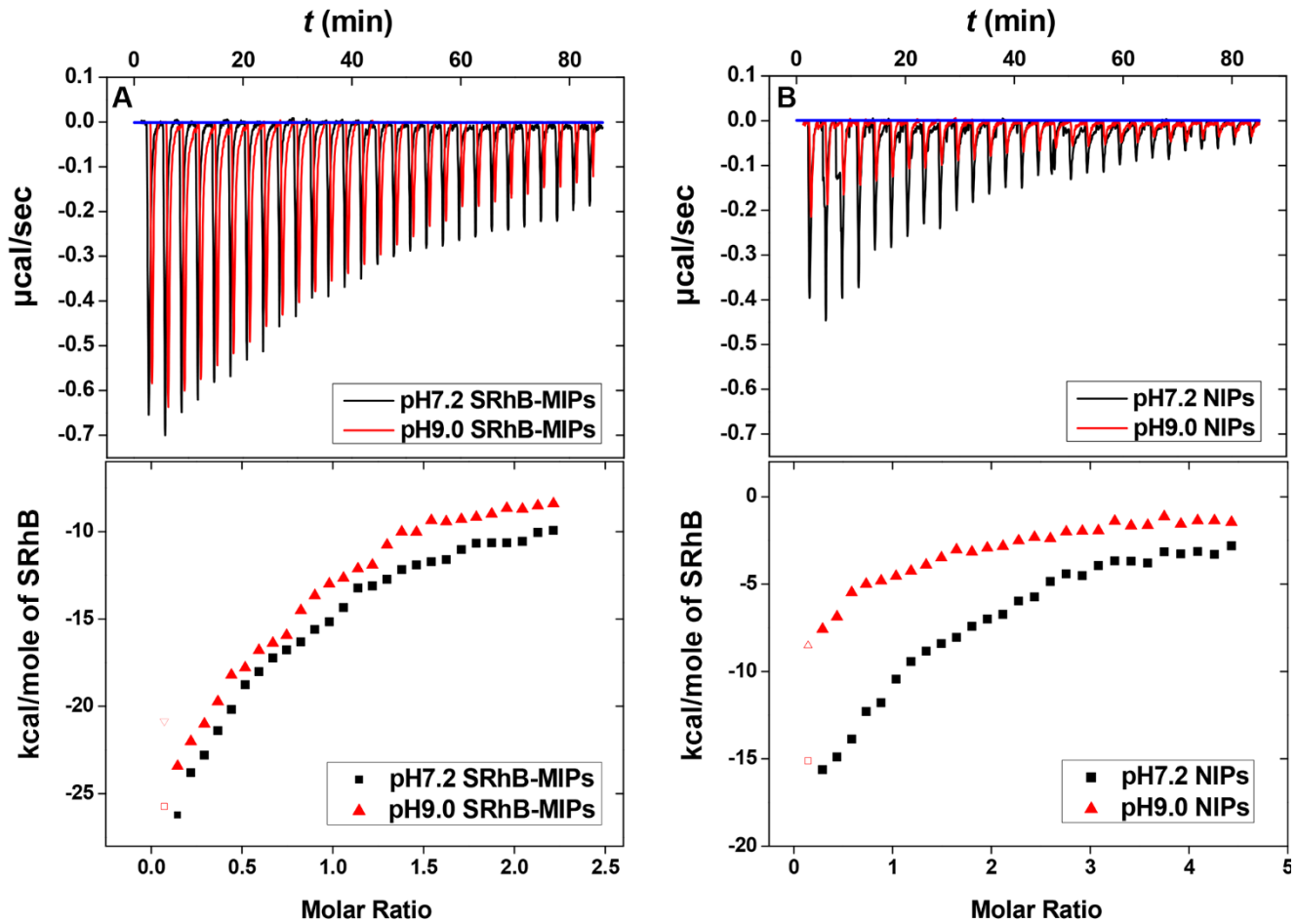


Figure 5. ITC titration curves obtained at 298.15 K for binding of SRhB-MIP nanogels (A) and NIP nanogels (B) for SRhB in 20 mM phosphate buffer at pH 7.2 or 9.0. The original titration traces and the integrated heat of each reaction are shown.

Table 2. ITC binding data for sulforhodamine-B to SRhB-MIPs and NIPs at pH 7.2 and 9.0 phosphate buffer ^a.

Nanogels	K_a ($\times 10^5 \text{ M}^{-1}$)	ΔG (kcal mol ⁻¹)	ΔH (kcal mol ⁻¹)	-TΔS (kcal mol ⁻¹)	N
SRhB-MIPs at pH7.2	0.47 ± 0.012	-6.4	-27.8 ± 0.4	21.4	1.0 ± 0.1
SRhB-MIPs at pH9.0	0.29 ± 0.005	-6.1	-26.1 ± 0.2	20.0	1.2 ± 0.2
NIPs at pH7.2	0.064 ± 0.007	-5.4	-17.7 ± 0.15	12.3	0.8 ± 0.1
NIPs at pH9.0	0.0031 ± 0.0006	-3.3	-8.3 ± 0.08	5.0	0.65 ± 0.1

^a The titrations were generally performed in duplicates and the errors between the runs were generally < 20%.

Binding isotherms

To further characterize gel binding, the adsorption isotherms of three nanogels were measured at pH 7.2. The experimental data could fit to the Langmuir binding model (Figure 6). The fitting to a Langmuir isotherm suggests that the binding is likely to be reversible and saturates at a monolayer capacity with just a single type of binding site. This supports our fitting of ITC data using a single type of binding site model. In all the cases, more adsorption was achieved with increasing of the target molecule concentration. The maximal adsorption by the SRhB-MIPs was higher than that by the fluorescein-MIPs and NIPs (Figure 6A), consistent with the IF difference. For adsorption of fluorescein (Figure 6B), the maximal adsorption amounts by three nanogels showed a bigger difference than those for SRhB, in which fluorescein-MIPs could reached at 15.8 μM while only around 6 μM for SRhB-MIPs and NIPs. The dissociation constant from the isothermal study is 22.3 μM (SRhB for its imprinted gels), which is consistent with the ITC-based measurement.

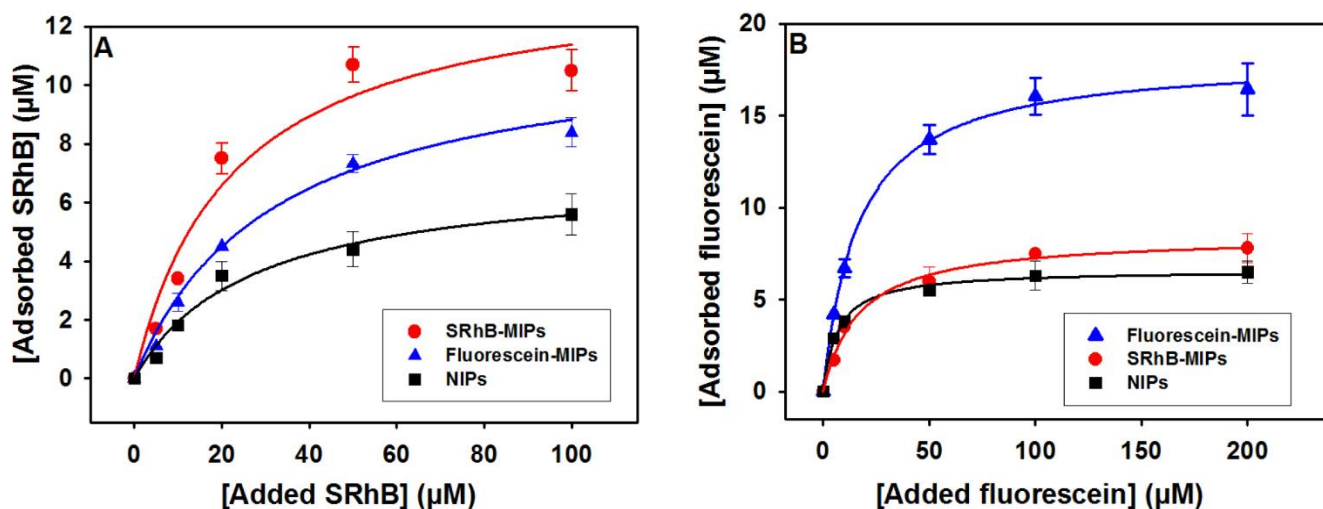


Figure 6. Adsorption isotherms of three nanogels (10mg/mL) rebinding for (A) SRhB and (B) fluorescein in 20 mM phosphate buffer (pH 7.2).

Conclusions

In this work, we prepared various types of nanogels by imprinting with SRhB, fluorescein, or without any template. The rebinding efficiency and IF for the MIPs were significantly affected by the buffer pH. At pH 9, non-specific electrostatic interactions between the template and SRhB-imprinted gels were reduced, allowing a drastically improved IF to 7.4. This improvement was not accompanied by a decrease in the binding capacity for the imprinted gels. ITC further determined the thermodynamic parameters for these different gels at different pH values, indicating the dominating enthalpy effect. This study indicates a promising way to engineer monomer composition and intermolecular forces for improving MIPs.

Acknowledgement

This work was supported by the Natural Sciences and Engineering Research Council of Canada (NSERC, STPGP 447472-13).

References

1. K. Ariga, H. Ito, J. P. Hill and H. Tsukube, *Chem. Soc. Rev.*, 2012, 41, 5800-5835.
2. S. Muyldermans, *Annu. Rev. Biochem.*, 2013, 82, 775-797.
3. J. Liu, Z. Cao and Y. Lu, *Chem. Rev.*, 2009, 109, 1948-1998.
4. M. Famulok, J. S. Hartig and G. Mayer, *Chem. Rev.*, 2007, 107, 3715-3743.
5. X. Fang and W. Tan, *Acc. Chem. Res.*, 2009, 43, 48-57.
6. L. Chen, S. Xu and J. Li, *Chem. Soc. Rev.*, 2011, 40, 2922-2942.
7. K. Haupt and K. Mosbach, *Chem. Rev.*, 2000, 100, 2495-2504.
8. G. Wulff, *Chem. Rev.*, 2002, 102, 1-28.
9. B. Sellergren, *Nature Chem.*, 2010, 2, 7-8.
10. N. N. M. Yusof, E. Tanioka and T. Kobayashi, *Sep. Purif. Technol.*, 2014, 122, 341-349.
11. J. Hou, H. Zhang, Q. Yang, M. Li, L. Jiang and Y. Song, *Small*, 2015.
12. N. A. Alenazi, E. P. Lai and J. M. Manthorpe, *J. Mol. Recognit.*, 2014, 27, 755-762.
13. Y. Sun, L. Jin, H. Wang and Y. Yang, *Soft Matter*, 2011, 7, 348-350.
14. A. Nematollahzadeh, W. Sun, C. S. Aureliano, D. Lütkemeyer, J. Stute, M. J. Abdekhodaie, A. Shojaei and B. Sellergren, *Angew. Chem.*, 2011, 123, 515-518.
15. M. E. Byrne and V. Salián, *Int. J. Pharm.*, 2008, 364, 188-212.
16. M. E. Byrne, K. Park and N. A. Peppas, *Adv. Drug Delivery Rev.*, 2002, 54, 149-161.

17. T. Miyata, M. Jige, T. Nakaminami and T. Urakami, *Proc. Natl. Acad. Sci. U. S. A.*, 2006, 103, 1190-1193.
18. Y. Hoshino, H. Koide, T. Urakami, H. Kanazawa, T. Kodama, N. Oku and K. J. Shea, *J. Am. Chem. Soc.*, 2010, 132, 6644-6645.
19. A. A. Volkert and A. J. Haes, *Analyst*, 2014, 139, 21-31.
20. M. J. Whitcombe, I. Chianella, L. Larcombe, S. A. Piletsky, J. Noble, R. Porter and A. Horgan, *Chem. Soc. Rev.*, 2011, 40, 1547-1571.
21. C. Wang, A. Javadi, M. Ghaffari and S. Gong, *Biomaterials*, 2010, 31, 4944-4951.
22. W. Zhang, X.-W. He, Y. Chen, W.-Y. Li and Y.-K. Zhang, *Biosens. Bioelectron.*, 2012, 31, 84-89.
23. G. Pan, Q. Guo, C. Cao, H. Yang and B. Li, *Soft Matter*, 2013, 9, 3840-3850.
24. J. Orozco, A. Cortés, G. Cheng, S. Sattayasamitsathit, W. Gao, X. Feng, Y. Shen and J. Wang, *J. Am. Chem. Soc.*, 2013, 135, 5336-5339.
25. L. Tan, C. Kang, S. Xu and Y. Tang, *Biosens. Bioelectron.*, 2013, 48, 216-223.
26. H. Taguchi, H. Sunayama, E. Takano, Y. Kitayama and T. Takeuchi, *Analyst*, 2015, 140, 1448-1452.
27. S. Des Azevedo, D. Lakshmi, I. Chianella, M. J. Whitcombe, K. Karim, P. K. Ivanova-Mitseva, S. Subrahmanyam and S. A. Piletsky, *Ind. Eng. Chem. Res.*, 2013, 52, 13917-13923.
28. M. Meng, Z. Wang, L. Ma, M. Zhang, J. Wang, X. Dai and Y. Yan, *Ind. Eng. Chem. Res.*, 2012, 51, 14915-14924.
29. L. I. Andersson, *Anal. Chem.*, 1996, 68, 111-117.
30. B. Sellergren and L. I. Andersson, *Methods*, 2000, 22, 92-106.
31. B. Sellergren and K. J. Shea, *J. Chromatogr., A*, 1993, 635, 31-49.

32. J. G. Karlsson, B. Karlsson, L. I. Andersson and I. A. Nicholls, *Analyst*, 2004, 129, 456-462.
33. B. E. Polat, S. Lin, J. D. Mendenhall, B. VanVeller, R. Langer and D. Blankschtein, *J. Phys. Chem. B*, 2011, 115, 1394-1402.
34. M. Kitamura, K. Murakami, K. Yamada, K. Kawai and M. Kunishima, *Dyes Pigm.*, 2013, 99, 588-593.
35. Z. Zhang, N. Chen, S. Li, M. R. Battig and Y. Wang, *J. Am. Chem. Soc.*, 2012, 134, 15716-15719.
36. J. Liu, *Soft Matter*, 2011, 7, 6757-6767.
37. J. Liu, H. Liu, H. Kang, M. Donovan, Z. Zhu and W. Tan, *Anal. Bioanal. Chem.*, 2012, 402, 187-194.
38. A. Khademhosseini and R. Langer, *Biomaterials*, 2007, 28, 5087-5092.
39. L. Ye, R. Weiss and K. Mosbach, *Macromolecules*, 2000, 33, 8239-8245.
40. Y. Hoshino, T. Kodama, Y. Okahata and K. J. Shea, *J. Am. Chem. Soc.*, 2008, 130, 15242-15243.
41. J. Wang, P. A. Cormack, D. C. Sherrington and E. Khoshdel, *Angew. Chem., Int. Ed.*, 2003, 42, 5336-5338.
42. S. De and R. Kundu, *J. Photochem. Photobiol., A*, 2011, 223, 71-81.
43. T. Kasnavia, D. Vu and D. A. Sabatini, *Groundwater*, 1999, 37, 376-381.
44. Y. Ono and T. Shikata, *J. Am. Chem. Soc.*, 2006, 128, 10030-10031.
45. D. Gutmayer, R. Thomann, U. Bakowsky and R. Schubert, *Biomacromolecules*, 2006, 7, 1422-1428.
46. F. L. Arbeloa, P. R. Ojeda and I. L. Arbeloa, *J. Lumin.*, 1989, 44, 105-112.
47. I. L. Arbeloa and P. R. Ojeda, *Chem. Phys. Lett.*, 1982, 87, 556-560.
48. J. E. Selwyn and J. I. Steinfeld, *J. Phys. Chem.*, 1972, 76, 762-774.

49. J. K. Awino and Y. Zhao, *Chem. Commun.*, 2014, 50, 5752-5755.
50. J. K. Awino and Y. Zhao, *Chem. Eur. J.*, 2015, 21, 655-661.
51. S. Striegler, *Anal. Chim. Acta*, 2005, 539, 91-95.
52. A. Weber, M. Dettling, H. Brunner and G. E. Tovar, *Macromol. Rapid Commun.*, 2002, 23, 824-828.